Title:

Radical-Enhanced Intersystem Crossing in Perylene-Oxoverdazyl Radical Dyads

Authors:

Muhammad Imran, Maria Taddei, Andrey A. Sukhanov, Laura Bussotti, Wenjun Ni, Paolo Foggi, Gagik G. Gurzadyan, Jianzhang Zhao, Mariangela Di Donato, and Violeta K. Voronkova

Manuscript

WILEY-VCH

Radical-Enhanced Intersystem Crossing in Perylene-Oxoverdazyl Radical Dyads

Muhammad Imran,[a] Maria Taddei,[b] Andrey A. Sukhanov,[c] Laura Bussotti,[b] Wenjun Ni,[e] Paolo Foggi,[b,d] Gagik G. Gurzadyan,[e] Jianzhang Zhao,*[a] Mariangela Di Donato,*[b,f] and Violeta K. Voronkova*[c]

Abstract: Attaching stable radicals to organic chromophores is an effective method to enhance the intersystem crossing (ISC) of the chromophores. Herein we prepared perylene-oxoverdazyl dyads either by directly connecting the two units or using an intervening phenyl spacer. We investigated the effect of the radical on the photophysical properties of perylene and observed strong fluorescence quenching due to radical enhanced ISC (REISC). Compared with a previously reported perylene-fused nitroxide radical compound (triplet lifetime, τ_T = 0.1 μs), these new adducts show a longer-lived triplet excited state (τ_T = 9.5 μs). Based on the singlet oxygen quantum yield (Φ_Δ = 7%) and study of the triplet state, we propose that the radical enhanced internal conversion also plays a role in the relaxation of the excited state. Femtosecond fluorescence up-conversion indicates a fast decay of the excited state (<1.0 ps), suggesting a strong spin-spin exchange interaction between the two units. Femtosecond transient absorption (fs-TA) spectra confirmed direct triplet state population (within 0.5 ps). Interestingly, by fs-TA spectra, we observed the interconversion of the two states ($D_1 \leftrightarrow Q_1$) at ~80 ps time scale. Time-resolved electron paramagnetic resonance (TREPR) spectral study confirmed the formation of the quartet sate, we observed triplet and quartet states simultaneously with weights of 0.7 and 0.3, respectively. This is attributed to two different conformations of the molecule at excited state. DFT computations showed that the interaction between radical and chromophore is ferromagnetic (J > 0, 0.05 ~ 0.10 eV).

[a]   Dr. M. Imran, Prof. J. Zhao
        State Key Laboratory of Fine Chemicals, School of Chemical
        Engineering, Dalian University of Technology, E-208 West
        Campus, 2 Ling Gong Road, Dalian 116024, (P.R. China)
        E-mail: zhaojzh@dlut.edu.cn

[b]   M. Taddei, Dr. L. Bussotti, Prof. P. Foggi and Dr. M. Di Donato
        LENS (European Laboratory for Non-Linear Spectroscopy)
        via N. Carrara 1, 50019 Sesto Fiorentino (Italy)
        E-mail: didonato@lens.unifi.it

[c]   Dr. A. A. Sukhanov, Prof. V. K. Voronkova
        Zavoisky Physical-Technical Institute, FRC Kazan Scientific Center
        of RAS, Kazan 420029 (Russia)
        E-mail: vio@kfti.knc.ru

[d]   Prof. P. Foggi
        Dipartimento di Chimica, Biologia e Biotecnologie.
        Università di Perugia. via Elce di Sotto 8, 06123 Perugia (Italy)

[e]   W. Ni and Prof. G. G. Gurzadyan
        Institute of Artificial Photosynthesis, State Key Laboratory of Fine
        Chemicals, Dalian University of Technology, 2 Ling-Gong Road,
        Dalian 116024 (P.R. China)

[f]   Dr. M. Di Donato
        ICCOM-CNR. via Madonna del Piano 10, 50019 Sesto Fiorentino
        (FI) (Italy)
        E-mail: didonato@lens.unifi.it

        Supporting information for this article is given via a link at the end
        of the document.

1. Introduction

The generation of long-lived triplet excited states has been a subject of long-standing interest.[1,2] Long-lived triplet excited states of organic molecules are pivotal for their applications, i.e. photocatalytic organic reactions,[3–5] photodynamic therapy (PDT)[6–10] and triplet-triplet annihilation upconversion.[11–15] Many approaches have been used to attain efficient intersystem crossing (ISC), such as the heavy atoms effect,[16,17] exciton coupling,[18] charge recombination,[19,20] and electron spin converter.[17,21–23] However, drawbacks exist for these methods, for instance, using the heavy atom effect to promote ISC is not always very effective.[24] Also, the synthesis of triplet photosensitizers that based on spin converter and exciton coupling is very demanding and it is often difficult to predict the ISC yield in these systems.

Several investigations have demonstrated that stable organic radicals can be used to enhance the ISC of a chromophore.[13,25–28] Fluorescence quenching by stable radicals has been known for a long time, and radical labeled fluorophores have been used as molecular probes for selective detection of paramagnetic species.[29,30] It is known that upon photoexcitation, these radical-containing organic molecules result in well-defined spin states that can be examined by time-resolved electron paramagnetic resonance (TREPR) spectroscopy.[7,25,31–33] The chromophore and radical spin states can mix via spin-spin exchange interactions (quantified by the J coupling term) to produce an excited doublet (S = 1/2) and quartet state (S = 3/2), facilitating the ISC of the chromophore, through the mechanism of radical enhanced ISC (REISC).[7,13,26,34–36]

An interesting aspect of these systems is that the ISC of the chromophore-radical dyad becomes an electron spin allowed process ($D_n^* \rightarrow D_1$ transition), as compared to the ISC of the pristine chromophore ($S_1 \rightarrow T_1$ transition). Moreover, the excited doublet state decays faster than the excited quartet state due to the conservation of the spin multiplicity. Several radical-chromophore adducts have been studied previously, such as the anthracene-verdazyl,[37] pyrene-verdazyl,[38] perylenebisimide-nitroxide,[25,39] bodipy-TEMPO[13,40] and naphthalenediimide (NDI)-TEMPO.[7] It has been found that the ISC efficiency (Φ_T) varies between 8 − 80 % and the triplet state lifetime is in the range of 0.54 − 62 μs. Although promising, these results show that several challenges still exist for the design of efficient triplet photosensitizers based on the REISC, for instance, to achieve strong absorption of visible light, efficient ISC and a long-lived triplet excited state.[17,23]

Previously, perylene (Pery) fused with a stable nitroxide (NO•) radical was studied to enhance ISC, but the resultant triplet state shows a lifetime of only 0.1 μs.[26] Recently, our group synthesized naphthalenediimide-verdazyl (NDI-Ver) dyads. These dyads show strong absorption of visible light (ε = 19000 M^{-1} cm^{-1} at 550 nm), and reasonable REISC upon photoexcitation (Φ_Δ = 26%). The formation of high spin states (doublet and quartet) was confirmed by nanosecond transient absorption spectroscopy, and a biexponential decay of the transient signal was observed (τ_T = 0.05 μs 77% and 2.5 μs 22%).[41]
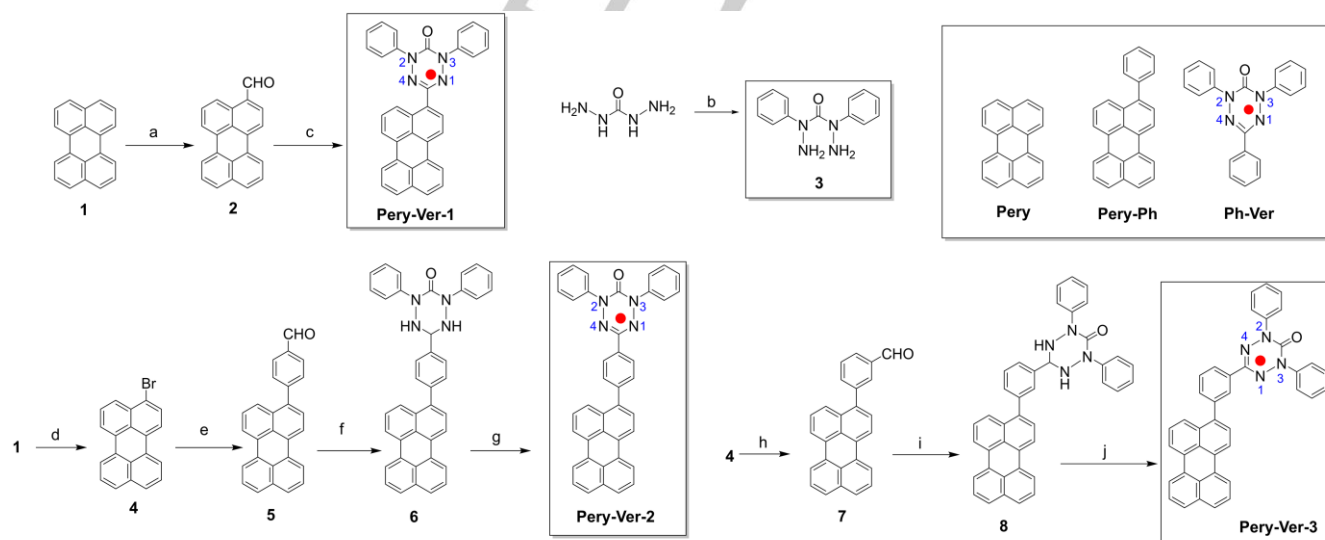
Inspired by these results, herein we linked the oxoverdazyl (Ver) radical to the perylene (Pery) chromophore and prepared three Pery-Ver dyads using different connections between the two units (**Pery-Ver-1, Pery-Ver-2** and **Pery-Ver-3**, Scheme 1). The perylene and radical units are directly connected in **Pery-Ver-1,** while an intervening phenyl ring has been introduced in both **Pery-Ver-2** and **Pery-Ver-3**. Different spectroscopic methods were employed to characterize the excited state kinetics of the systems, such as steady-state and femtosecond fluorescence up-conversion, cyclic voltammetry (CV), time-resolved femtosecond/nanosecond transient absorption (fs-TA and ns-TA) and TREPR spectroscopy. Furthermore, density functional theory (DFT) calculations were also performed to clarify the nature of the excited state of the systems.

2. Results and Discussion

2.1. Molecular Structure Design and Synthesis

Perylene is known for its high fluorescence quantum yield (up to Φ_F = 94%) and negligible ISC ability,[25,42,43] and is thus an ideal chromophore to be linked with a stable radical to study the REISC mechanism. We selected oxoverdazyl radical as the spin carrier and synthesized three radical compounds (**Pery-Ver-1, Pery-Ver-2** and **Pery-Ver-3,** scheme 1). In **Pery-Ver-1**, the perylene and radical are directly linked via a single C−C bond, so that we expect a strong spin-spin interaction. To increase the distance between radical and chromophore in **Pery-Ver-2** and **Pery-Ver-3,** a phenyl ring has been introduced between the two moieties, at 4-C and 3-C positions of the phenyl moiety, respectively, to reduce the interaction between the radical unit and the perylene chromophore, thus longer triplet state lifetime is anticipated.

The radical compounds were prepared using a modified literature method,[30] and the synthesis was carried out in two steps, involving first the condensation of perylene aldehyde with 2,4-diphenylcarbohydrazide and then the oxidation with 1,4-benzoquinone to obtain the verdazyl radical (Scheme 1). For **Pery-Ver-1**, the oxidation was carried out without prior isolation of the intermediate product. **Pery-Ph** and **Ph-Ver** were synthesized as reference compounds. All the radical compounds were obtained in moderate yields (see experimental section). For paramagnetic species (all the radical compounds) we were unable to obtain satisfactory ^{1}H NMR spectra. The molecular structures were verified by HRMS, FTIR, ESR

Scheme 1. Synthesis of the verdazyl radical labeled perylene compounds. (a) *o*-dichlorobenzene, POCl$_3$, DMF, stirred at 100 °C, for 4 h, under N$_2$, yield: 64%; (b) Carbohydrazide, CuI, iodobenzene, K$_3$PO$_4$, 1,10-phenanthroline, dry DMF, stirred at 90 °C, for 24 h, under N$_2$, yield: 38.4%; (c) i. compound **3**, pyridinium *p*-toluenesulfonate, dry MeOH, stirred at 70 °C, for 2 h, under N$_2$, ii. *p*-benzoquinone, dry toluene, heated at 80 °C, for 1 h, yield: 27%; (d) NBS, DMF, overnight at RT, under N$_2$, yield: 84%; (e) 4-formylphenylboronic acid, K$_2$CO$_3$, Pd(pph$_3$)$_4$, EtOH/ toluene/ H$_2$O (2:2:1 v/v/v), heated at 80 °C, under N$_2$, for 8 h, yield: 64.2%; (f) compound **3**, pyridinium *p*-toluenesulfonate, dry MeOH, stirred at 70 °C, under N$_2$, for 3 h, yield: 40%; (g) *p*-benzoquinone, dry toluene, heated at 80 °C, for 1.5 h, yield: 31.4%; (h) 3-formylphenylboronic, similar as step e), yield: 60.2%; (i) similar as step f), yield: 37%; (j) similar as step g), yield: 34.6%.

spectral and elemental analysis (CHN). All the data are presented in the Supporting Information.

2.2. UV/Vis Absorption and Fluorescence Emission Spectra

The UV/Vis absorption spectra of the compounds were studied (Figure 1). For **Pery-Ver-1,** characteristic absorption band centered at 451 nm with a strong vibronic progression is assigned to the $\pi-\pi^*$ transition of perylene. A broad tail at the red end of the band was observed, whichi is attributed to the verdazyl radical. The reference compound **Ph-Ver** shows two absorption bands centered at 567 and 320 nm, respectively (Figure 1). For the other two dyads, **Pery-Ver-2** and **Pery-Ver-3,** the absorption peaks of the perylene unit are at 449 and 447 nm respectively, slightly blue-shifted in comparison with **Pery-Ver-1** and **Pery-Ph**. The absorption band of verdazyl is also noted at about 570 nm, although with smaller molar absorption coefficients ($\varepsilon = 1200$ M^{-1} cm^{-1} at 570 nm) compared to **Ph-Ver** ($\varepsilon = 34000$ M^{-1} cm^{-1} at 567 nm), indicating a limited interaction among perylene and the radical at the ground state.

The pristine perylene shows a strong emission band centered at 445 nm (Figure 2a) with a fluorescence quantum yield of 94% (in toluene, Table 1). The fluorescence emission of **Pery-Ver-1** is almost completely quenched (Figure 2a), even in the non-polar solvent toluene. The fluorescence spectra of the dyads were also measured in solvents of different polarities, the results indicated that the emission is quenched in all solvents compared with the pristine perylene (Figure S24 and S25 in the Supporting Information). The strong quenching of the perylene fluorescence in the dyads can be ascribed to different reasons, including Förster Resonance Energy Transfer (FRET) towards the verdazyl moiety, photoinduced electron transfer (PET), spin-spin exchange interactions to form high spin states or radical enhanced ISC.[7,41,44–46]

Considering that the fluorescence of the radical dyads is
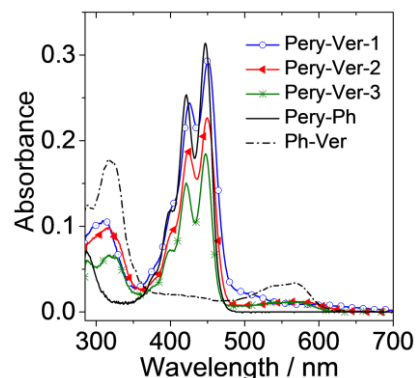
Figure 1. UV/Vis absorption spectra of the compounds. $c = 1.0 \times 10^{-5}$ M, in toluene, 20 °C.

also quenched in low polarity solvents, the occurrence of charge separation is unlikely. The occurrence of FRET can't be excluded, considering that the fluorescence of the perylene partially overlaps with the verdazyl absorption, however, because of the small molar absorption coefficient (ε) of the verdazyl radical and the poor spectral overlap, the process is expected to be non-efficient.
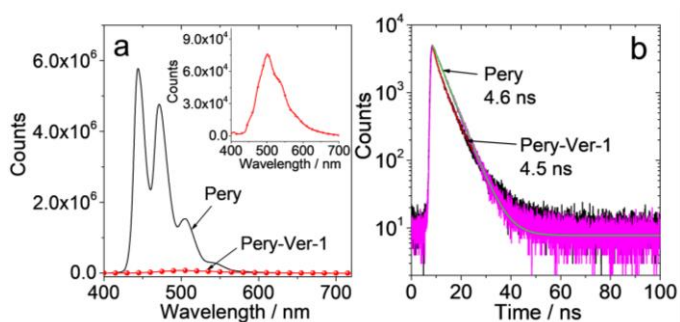
The fluorescence lifetime of **Pery-Ver-1** was measured using the time-correlated single-photon counting (TCSPC) technique (Figure 2b). The fluorescence decay can be fitted with a mono-exponential function, yielding a lifetime of 4.5 ns. In case of perylene and **Pery-Ph**, the fluorescence lifetimes are 4.6 ns and 4.0 ns, respectively (Table 1). Similar results were obtained for **Pery-Ver-2** and **Pery-Ver-3** (Figure S26 in the Supporting Information).

The singlet oxygen ($^1O_2$) quantum yields (Φ_Δ) of the dyads and the data are summarized in Table 1. For **Pery-Ver-1** and **Pery-Ver-2**, $\Phi_\Delta = 7$ and 4% were observed, respectively (in *n*-hexane). However, no $^1O_2$ production was observed for **Pery-Ver-3**. To go further insight into the fluorescence quenching mechanism, the fluorescence up-conversion study was performed to track the decay kinetics at the femtosecond timescale (See next section for detail).

Table 1. Photophysical properties of the compounds [a]

Compounds	λ_{abs} /nm[b]	ε[c]	λ_{em}/nm[d]	Φ_F/%[e]	τ_F /ns[f]	Φ_Δ/%[g]	τ_T /μs[h]
Pery-Ver-1	451/500	2.94/0.22	510	0.91 ± 0.02	4.5 ± 0.1	7 ± 0.2	9.5 ± 0.1
Pery-Ver-2	449/570	2.27/0.12	474	1.25 ± 0.1	2.8 ± 0.1	4 ± 0.2	7.8, 1.6 ± 0.1
Pery-Ver-3	447/570	1.85/0.12	464	1.58 ± 0.1	3.8 ± 0.1	—[j]	—[j]
Perylene	438	2.98	445	94 ± 0.5	4.6 ± 0.1	—[j]	41[i]
Pery-Ph	447	3.14	462	90 ± 0.4	4.0 ± 0.1	—[j]	—[j]
Ph-Ver	567	0.34	—[k]	—[k]	—[k]	—[k]	—[k]

[a] In toluene (1.0 × 10^{-5} M). [b] Absorption maxima. [c] Molar absorption coefficient (10^4 M^{-1} cm^{-1}). [d] Fluorescence emission maxima. [e] Fluorescence quantum yields with perylene (Φ_F = 94%, *n*-hexane) as the standard, in toluene. [f] Fluorescence lifetimes, in DCM. [g] Singlet oxygen quantum yield (Φ_Δ) with Ru(bpy)$_3$[PF$_6$]$_2$ as standard (Φ_Δ = 57% in DCM) in *n*-hexane. [h] Triplet state lifetime measured by nanosecond transient absorption in deaerated *n*-hexane. [i] By intermolecular TTET method. [j] Not observed. [k] Not applicable.

Figure 2. Fluorescence emission spectra in optically matched solution of (a) perylene and **Pery-Ver-1**, λ_{ex} = 390 nm, A = 0.10; (b) Fluorescence lifetime decay curve of perylene λ_{ex} = 400 nm at 440 nm) and **Pery-Ver-1** (λ_{ex} = 445 nm at 503 nm). Inset in (a) show magnified view of quenched fluorescence of **Pery-Ver-1**. c = 1.0 × 10^{-5} M, in toluene, 20 °C.

2.3. Femtosecond Fluorescence Up-Conversion Spectroscopy: Ultrafast Spin-SpinInteraction

Fluorescence up-conversion is a useful technique to detect short-living emissive excited state.[47–49] The time-resolved femtosecond fluorescence up-conversion spectra of the dyads are shown in Figure 3. In case of the reference perylene (Figure S27 in the Supporting Information), two decay components are obtained τ_1 = 39 ps (31%), which can be ascribed to a vibrational relaxation process and τ_2 = 4.6 ns (69%), which is a normal fluorescence decay.

For **Pery-Ver-1,** three components are obtained, the first one with ultrashort lifetime τ_1 = 0.59 ps, has a significant amplitude of 38% (Figure 3a). This ultrafast fluorescence decay is attributed to the quenching effect due to electron spin-spin interaction. The time scale of the second decay component is τ_2 = 62 ps (35%), attributed to a vibrational or structural relaxation of the emissive state which is also evident in femtosecond transient absorption spectra (fs-TA section). The longer time component, τ_3 = 4.5 ns with amplitude of 27%, in agreement with the TCSPC data, is attributed to fluorescence decay. Similarly, three-time components were also observed for the other two dyads. For **Per-Ver-2**, the obtained lifetimes are τ_1 = 0.78 ps (67%), τ_2 = 63 ps (20%) and τ_3 = 2.8 ns (13%), respectively (Figure

3b). For **Pery-Ver-3** (Figure 3c), the amplitude of the fast decay component is also significant, which is about 55%. This result confirms that, the radiative decay accounts only for a limited part of the excited-state deactivation of the dyads.

2.4. CW-EPR Spectroscopy: Electronic Ground State of Dyads

The room temperature continuous-waves electron paramagnetic resonance (CW-EPR) spectra in degassed dichloromethane were studied (Figure 4). The solution EPR spectra were well analyzed by spectral simulation, all the compounds showed typical lineshapes of verdazyl radical (nine-lines hyperfine pattern). The simulation data revealed that EPR spectra are dominated by hyperfine coupling (hfc) with two distinct sets of two nitrogen atoms, which are not equivalent in pairs. These results are in agreement with previously reported verdazyl radicals.[30]

Furthermore, the electronic ground state of all dyads is a doublet state (S = 1/2) and the *g* factors calculated from the ESR data are 2.00385 similar for all the dyads, which are very close to that of **Ph-Ver** (*g* = 2.00386). This result indicates that the electronic structures of verdazyl moiety in the radical-containing dyads (**Pery-Ver-1**, **Pery-Ver-2** and **Pery-Ver-3**) are close to that of the isolated phenylverdazyl (**Ph-Ver**).

For the simulation of CW-EPR spectra, the following spin Hamiltonian model was used (Eq. 1)

$$H = g\mu_\beta S + \sum_{i=1}^{2} A_{N1}SI + \sum_{i=1}^{2} A_{N2}SI \qquad \text{(Eq. 1)}$$

where S = 1/2, I = 1.

Furthermore, we also did quantum chemical calculations to estimate the hyperfine coupling constants. For **Pery-Ver-1**, the computed isotropic hyperfine coupling constants are 20.28 and 20.01 in MHz for the two nitrogen atoms of radical sites (1N and 4N atoms) and 12.56 and 12.37 in MHz for the two adjacent nitrogen atoms (2N and 3N atoms). These results suggest that the four N atoms of verdazyl moiety are in sets of two non-equivalent N atoms in the dyads. Moreover, our experimental and theoretical
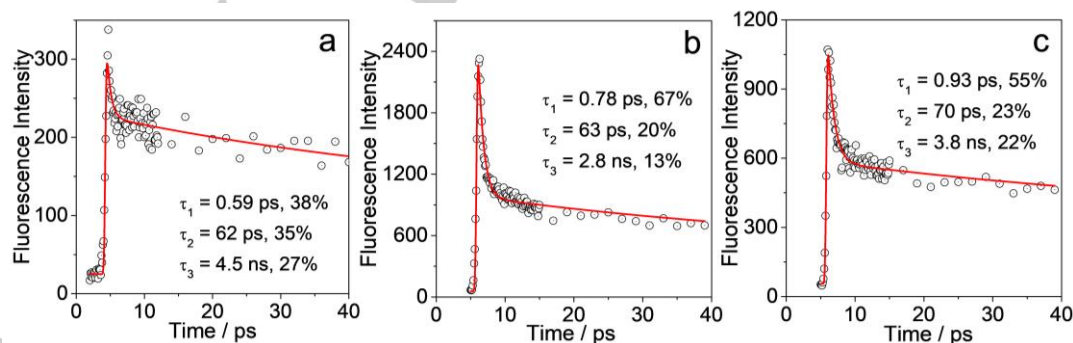

Figure 3. Femtosecond fluorescence up-conversion decay traces of (a) **Pery-Ver-1**, at 508 nm; (b) **Pery-Ver-2**, at 470 nm and (c) **Pery-Ver-3**, at 463 nm, λ_{ex} = 400 nm. c = 1.4 × 10^{-5} M, in toluene, 20 °C.

Table 2. Calculated and experimentally obtained CW-ESR parameters of the compounds

Compounds	Frequency (GHz)	g value [a]	[$A_{N2,3}$, $A_{N1,4}$] [b] (MHz)	A_{iso} in MHz [c]			
				1N	2N	3N	4N
Pery-Ver-1	9.5265	2.00385	[12.8, 18.2]	20.2	12.6	12.4	20.0
Pery-Ver-2	9.5265	2.00385	[12.7, 18.2]	19.9	12.5	12.4	20.0
Pery-Ver-3	9.5258	2.00385	[12.9, 18.2]	20.0	12.4	12.5	20.0
Ph-Ver	9.5274	2.00386	[12.5, 18]	19.8	12.6	12.4	19.3

[a] g factor, the error did not exceed 0.001%. [b] Hyperfine coupling constants obtained after stimulation of CW-EPR spectra. [c] Isotropic hyperfine coupling constants calculated by DFT.
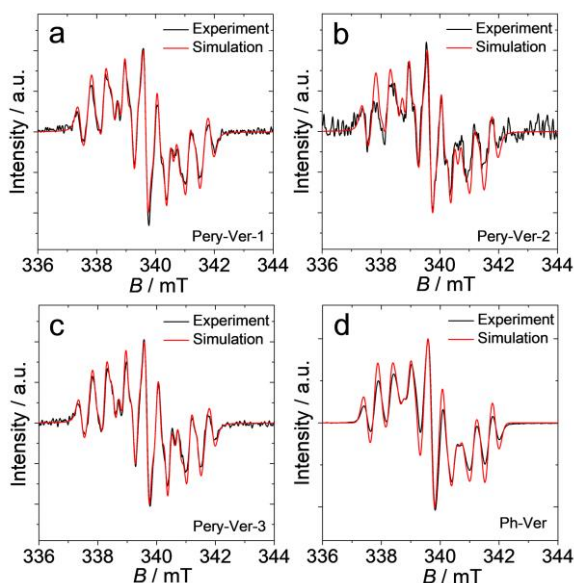
Figure 4. ESR spectra of (a) **Pery-Ver-1**; (b) **Pery-Ver-2**; (c) **Pery-Ver-3** and (d) **Ph-Ver.** c = ca. 1.0×10^{-4} M, in deaerated DCM, 20 °C.

results agree with the previously reported data of verdazyl with hyperfine coupling constants of 18.2 MHz for radical site nitrogen atoms and 14.8 MHz for two other adjacent nitrogen atoms.[33,50] The spin-density distribution over the four nitrogen atoms further supports this conclusion (vide infra). A similar trend was observed for the other two dyads (**Pery-Ver-2** and **Pery-Ver-3**). The complete EPR spectral parameters are summarized in Table 2.

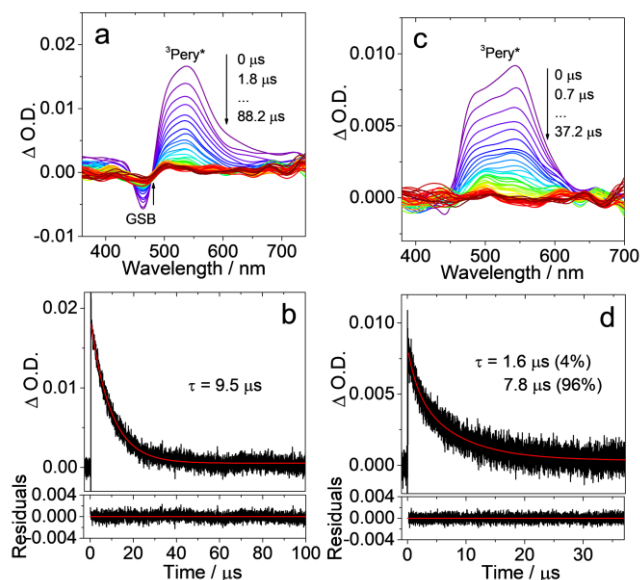**2.5. Nanosecond Transient Absorption Spectroscopy: Triplet Excites States of the Dyads**

In order to verify the triplet production of the radical containing dyads, nanosecond time-resolved transient absorption (ns-TA) spectra were recorded (Figure 5). For **Pery-Ver-1,** an excited state absorption (ESA) band in the region from 480 to 600 nm was observed upon nanosecond pulsed laser excitation (Figure 5a). The negative signal at about 464 nm is assigned as the ground state bleach (GSB) band. The lifetime of transient species was determined as 9.5 μs in deaerated solution by monitoring the decay trace at 540 nm (Figure 5b). The lifetime is reduced to 0.06 μs in

aerated solution (Figure. S29, Supporting Information).

For **Pery-Ver-2**, a broader ESA band was observed in the range of 450 – 600 nm. The GSB band at 450 nm overlaps with the ESA band (Figure 5c). The observed ESA bands in both radical dyads could be assigned to triplet excited state of the perylene chromophore ($T_1 \rightarrow T_n$ transition). However, these bands are broader with full-width-at-half-maximum (FWHM) of 4277 cm^{-1} compared to that previously observed for the perylene-NO$^{\bullet}$ dyad or perylene-bodipy donor/acceptor dyads (with FWHM of about 2176 ~ 2191 cm^{-1}.[26,51] A reason for this observation could be the presence of π-conjugation between the stable radical and the chromophore, which modify the spin distribution of the dyads compared to the isolated perylene. Modifications of the triplet band-shape, involving a red-shift have been previously reported in case of anthracene-verdazyl radical.[27]

To further confirm the triplet state formation in the radical dyads, we used a triplet-triplet energy transfer (TTET) method to populate the triplet state of the perylene, by using the reduced form of the radical-perylene compounds, i.e. compounds **6** and **8** (Scheme 1) as triplet energy acceptors and 2,6-diiodoBodipy as triplet energy donor. In this case, an ESA band was observed in the ns-TA spectra, ranging up to 550 nm, which is broader as compared to the triplet ESA of native perylene. The biphasic evolution of the transient signal at 520 nm indicates the TTET process from the donor to the acceptor (Figure S31−S33, Supporting Information).

For compound **6**, by fitting the kinetic trace at 480 nm, a triplet lifetime of 108 μs was obtained (global fitting analysis is given in Figure S33, Supporting Information). This lifetime is much longer than that of **Pery-Ver-1**. We attribute the short triplet state lifetime in **Pery-Ver-1** to the electron spin-spin interaction between the verdazyl radical and the chromophore. Compared with the TTET experiment with pristine perylene as energy acceptor (Figure S34, Supporting Information), the triplet ESA band observed with compounds **6** and **8** after TTET is much broader, further suggesting that the band broadening observed for the perylene-verdazyl dyads can be ascribed to the presence of π-conjugation between the two moieties.

Figure 5. Nanosecond time-resolved transient absorption spectra of the radical-containing compounds. (a) **Pery-Ver-1** upon pulsed laser excitation (c = 2.0 × 10^{-5} M); (b) decay trace at 540 nm. (c) **Pery-Ver-2** (c = 3.0 × 10^{-5} M); (d) decay trace at 540 nm. λ_{ex} = 445 nm. In deaerated n-hexane, 20 °C.

The triplet state lifetime of **Pery-Ver-2** was determined by monitoring the decay trace at 540 nm (Figure 5d), and a biexponential decay was observed, with lifetimes of 1.6 μs (4%) and 7.8 μs (96%). We propose that the two decay components could be due to two different states. Previously biexponential decay was observed for NDI-verdazyl dyads.[41] The triplet state lifetimes observed for the Pery-Ver dyads are much longer than that previously reported for the fused perylene-NO• radical compound (τ_T = 0.1 μs) [26] and the perylenediimide-nitroxide radical (τ_T = 0.35 ~ 8.4 μs).[25] Short triplet lifetime were observed for other chromophore-radical dyads, e.g. perylenebisimide-TEMPO (τ_T = <1.0 μs) and phthalocyaninatosilicon-nitroxide (τ_T = 0.86 ~ 7.6 μs) radical compounds.[52,53] Recently, our group studied NDI-TEMPO (τ_T = 8.7 μs) and NDI-Verdazyl (τ_1 = 0.05 and τ_2 = 2.5 μs) dyads, which also show similarly short triplet lifetimes.[7,41]

Although the triplet lifetime observed in this case is longer compared to other chromophore-radical dyads, it is still much shorter than that accessed by heavy atom effect in 3-bromoperylene (ca. 62 μs) or obtained by an electron donor/acceptor approach in perylene-phenothiazine dyads (ca. 156 ~ 223 μs).[51,54] This observation is reasonable because it is well known that stable radicals can quench the triplet state to large extent.[55,56] Indeed, since the full spin multiplicity of the dyad with the perylene in its triplet state can be either a doublet or quartet, the deactivation of the excited doublet state becomes a partially spin allowed process.

For **Pery-Ver-3**, we did not observe triplet signals in the ns-TA spectral measurements, although the formation of triplet states is evident from the ultrafast transient absorption data (see fs-TA section). This can imply that the triplet lifetime is shorter than the instrument response function (IRF) of the ns-TA spectrometer (< 10 ns).

2.6. Femtosecond Transient Absorption Spectroscopy: Ultrafast Direct REISC

To elucidate the timescale of triplet state formation, the femtosecond transient absorption (fs-TA) spectra of the dyads were measured (Figure 6). The data were analyzed with single value decomposition (SVD) and global fitting and target analysis, employing a linear unidirectional decay scheme, obtaining the time constants and the Evolution Associated Difference Spectra (EADS). In previously reported radical-containing molecules, for instance, NDI labeled with TEMPO, the ISC occurs within 338 ps,[7] whereas for the NDI-veradazyl dyad a charge recombination-induced ISC was observed (time constant: 1.40 ps), instead of the expected electron spin-spin exchange interaction-induced ISC.[41] Furthermore, in the compact perylene-NO• dyad, the REISC takes place within 1 ps.[26] These results indicate that in radical labeled molecular systems, ISC can be fast and can occur either through the formation of a CS state or by direct REISC.

On the basis of experimental data and predicted excited state energy, 400 nm photoexcitation would lead to populating higher excited state (D_n) instead of D_2. In this case, it would be D_3 as predicted by TD-DFT (Table S2, Supporting Information).[57] From the D_3 state, either an ultrafast internal conversion (IC) towards the D_2 state or REISC can occur. IC towards D_2 cannot be resolved by transient absorption spectroscopy, possibly because occurring at a time scale faster than the time resolution of the measurement, herein we observed the direct REISC in the sub-picosecond timescale. The initial EADS obtained from global analysis for **Pery-Ver-1** shows the typical perylene GSB band in the range of 425−450 nm. In addition, an intense transient absorption band centered at about 700 nm, assigned as the $S_1 \rightarrow S_n$ transition of the perylene moiety, is observed (Figure 6a).[58,59] On an ultrashort time scale of 0.5 ps, the 700 nm band decays and a new ESA band appears at about 500 nm (red line in Figure 6a). The new ESA is very similar to the band assigned to the triplet excited state of perylene, and it presents a broad red tail that well matches with the ns-TA spectra (Figure 5a), lacking in the case of the pristine chromophore.

This observation implies the occurrence of ultrafast REISC in the dyad, with the formation of the perylene triplet state within 0.5 ps, promoted by the verdazyl radical. Ultrafast spin-spin exchange interaction between perylene and verdazyl radical could be the reason for this observation. The intensity of the transient absorption
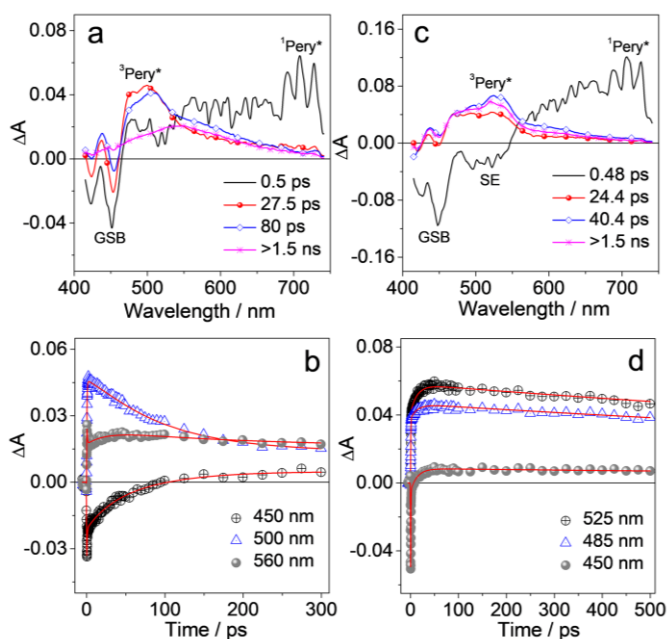
Figure 6. Evolution associated difference spectra (EADS) obtained from global analysis of fs-TA data recorded for (a) **Pery-Ver-1**; (b) respective kinetic traces at 450, 500 and 560 nm. (c) **Pery-Ver-2**; (d) respective kinetic traces at 450, 485 and 525 nm. λ_{ex} = 400 nm. In toluene.

peak at 500 nm decreases on its blue side and slightly rises on its red side within 27.5 ps (evolution from the red to blue EADS in Figure 6a). A substantial decrease in intensity is then observed within 80 ps. The long-living spectral component presents a broad peak at about 550 nm, and the ESA shape appears similar to that observed in the ns-TA spectra (Figure 5a).

The evolution observed on the 80 ps timescale could be due to the transition between two different states. In principle, both doublet and quartet states can be formed by ISC for this radical dyad, which could interconvert among each other in case of strong exchange interactions (note the D_1 state and the Q_1 state share almost similar energy). Although the perylene unit is in a triplet state in both D_1 and Q_1, the spin density distribution could partially change in these two states, so that different excited state absorption bands could be associated with the $D_1 \rightarrow D_n$ and $Q_1 \rightarrow Q_n$ transitions. Furthermore, while the transition from the D_n excited state reached upon photoexcitation towards D_1 is partially spin allowed, the transition towards Q_1 is a spin forbidden process, thus expected to be slower.

The dynamics observed on the 80 ps timescale could thus reflect interconversion and equilibration among the two states ($D_1 \leftrightarrow Q_1$) produced by REISC. The decrease of intensity at 500 nm and increase of intensity at 560 nm on the <100 ps timescale is well noticed by looking at the kinetic traces in Figure 6b.

For **Pery-Ver-2**, an intervening phenyl spacer is present

between the two units. Also, in this case a GSB at about 450 nm and an intense transient absorption band at 700 nm, along with a stimulated emission band peaking at about 520 nm are observed in the initial spectral component (black line in Figure 6c). These signals can all be attributed to the perylene singlet excited state.[58] Within about 0.48 ps the ESA assigned to the perylene singlet decays, and a new broad ESA band appears, once again indicating the ultrafast direct ISC. The triplet ESA observed for **Pery-Ver-2** is quite broad, extending in the range from 430 nm to 550 nm. The intensity of the triplet signal increases on the 24.4 ps time scale (evolution from red to blue line, Figure 6c), comparatively more on its red side than the blue side, signaling a biphasic triplet formation. The triplet signal then slightly decreases on the following 40.4 ps timescale. The lifetime of the last spectral component is beyond the maximum pump-probe delay accessible with the instrument (>1.5 ns), an accurate triplet lifetime has been provided in the previous section by ns TA spectroscopy. In case of this dyad, the final spectrum is slightly different compared with the shape of the triplet ESA registered with ns-TA spectroscopy (Figure 5c) which could be due to the occurrence of different transitions of doublet and quartet states at the shorter timescale. The kinetic traces at selected wavelengths are given in Figure 6d.

The evolution of the transient signal measured for **Pery-Ver-3** (Figure S35 in the Supporting Information) is almost similar to that observed for **Pery-Ver-2.** Also in this case, a GSB band at about 450 nm and the perylene singlet excited state absorption band at about 700 nm are present in the initial spectral component. Again, the ISC appears as a biphasic process and is signaled by the appearance of a very broad triplet ESA band peaking at about 510 nm, rising with an ultrafast component of about 0.6 ps, and a slower component of about 25 ps. The intensity of the triplet signal partially decreases on the following 470 ps timescale. The lifetime of the last spectral component can be fitted as 7.3 ns which is well beyond the maximum accessible pump-probe delay (1.5 ns). The decay traces at 450 nm and 510 nm are reported in Supporting Information Figure S35.

2.7. Time-Resolved EPR Spectroscopy: Observation of High Spin Quartet State

To further investigate the spin dynamics of the radical-containing dyads, the TREPR spectra of **Pery-Ver-1** in frozen solution are presented in Figure 7. After 450 nm laser flash, a spectrum with both absorptive and emissive (*a/e*) polarization pattern was observed. The spectra are not typical triplet or quartet state spectra, two main peaks at 315 mT and 375 mT were observed (Figure 7a). The intensity of the signals has a different time dependence.

The spectral simulation indicates that the TREPR spectrum is a sum of two spectra due to two spin states, i.e. the triplet excited state of perylene (T_1) and excited quartet state (Q_1). At

initial delay times, the overlaid spectra from both triplet and quartet states were observed. The spectrum simulated at 600 ns delay time contains both the states as the sum of triplet state spectrum and quartet state spectrum with weights of 0.7 and 0.3, respectively (Figure 7b). At longer delay times, the spectrum mainly arises from the triplet state, which persists up to the microsecond timescale. The TREPR spectrum and the simulation at 3.5 µs are given in Figure 7c, and represent the typical TREPR spectrum of perylene triplet state.[54] For the observed quartet state the electron spin polarization (ESP) pattern is almost similar as observed for pyrene-verdazyl compound, but it is opposite to that of the perylene-NO• dyad.[26,38]

The TREPR spectrum was fitted by computer simulation and the obtained parameters are compiled in Table 3. For the quartet state, the zero-field splitting (ZFS) parameters were determined as $|D|$ = 675 MHz and $|E|$ = 160 MHz, with g = 2.002. The relative population (polarization) of the M_s sublevels determined as $P(-1/2)$ = 1, $P(1/2)$ = 1, $P(-3/2)$ = 0 and $P(3/2)$ = 0. The D value is smaller than that observed previously for the Q_1 state of perylene-NO• (750.4 MHz). This discrepancy may be due to the mixing of triplet character into the quartet state. On the other hand, for the triplet state, the ZFS parameters were determined as $|D|$ = 1575 MHz and $|E|$ = 80 MHz with g = 2.007. The population of the sublevels of the triplet state are P_x = 0.87, P_y = 0.13 and P_z = 0. These values are close to the results reported previously for compact donor-acceptor dyads, the ZFS $|D|$ = 1630 MHz and $|E|$ = 68 MHz.[54]

For the D_1 state, the spin-allowed nature of the transition may lead to a faster decay towards D_0. That could be the reason why we did not observe any signal arising from the D_1 state in the TREPR investigation. On the other hand, Q_1 can be easily observed due to the spin forbidden nature of the state, but the observation of the triplet state is unusual. There was no decomposition during the TREPR measurements, which was confirmed by the fact that the signals remained identical when repeating the experiments. We also did not observe any spectral change before and after ns-TA measurements. Previously, both quartet and triplet states in TREPR spectrum were observed for zinc-tetraphenylporphinato (ZnTPP) complexes coordinated by

an axial ligand containing a nitroxide radical.[60] It was proposed that two conformations of the molecule contribute to this observation. Weak electron exchange interaction was observed for the dyad containing PBI-TEMPO, which showed the triplet state.[52] In a compact ring fused perylene-NO• dyad, however only the quartet state was observed.[26] The ESP phase pattern of the quartet state spectrum of **Pery-Ver-1** is similar to that previously reported for 9-anthracne-(4-phenylverdazyl) radical, but no triplet state was observed for that dyad.[61] Moreover, the quartet state spectrum of **Pery-Ver-1** is also almost similar as observed for the quartet state of anthracene-verdazyl dyad or anthraquinone-anthracene-verdazyl triad.[33]

In this case, the observation of excited triplet state together with quartet state could be due to different geometries of **Pery-Ver-1** at the excited state, which is supported by the computation of potential energy curves (Figure 10). However, the assessment of this statement requires additional research in the future. The individual simulated spectra of both the states (quartet and triplet) are given in Figure 8. To assign the spin multiplicity of the TREPR spectra, nutation frequencies were determined by echo-detected transient nutation, the nutation frequencies for the spin quantum numbers of S = 3/2 and 1/2 are different (Figure S36 in the Supporting Information). No TREPR signal was observed for the other two dyads due to poor ISC ability, although we observed ns-TA and fs-TA signals for **Pery-Ver-2** and fs-TA spectra for **Pery-Ver-3.**

2.8. Density Functional Theory Calculations: Doublet and Quartet State Geometries and Spin Density Distribution

Firstly, we optimized the geometries of the dyads at ground doublet (D_0) and excited Quartet (Q_1) states and determined the dihedral angles between the perylene and verdazyl units. For **Per-Ver-1**, the dihedral angle between perylene and the directly connected radical moiety is 42.6° at the D_0 state and it is reduced to 25.7° for the excited Q_1 state (Figure 9). **For Per-Ver-2**, the angle between perylene and phenyl ring attached to verdazyl is 52.3° at D_0 state and 45.3° at Q_1 state, while on radical side (between phenyl ring and verdazyl unit) the dihedral angle is 4.9° and 0.9° at D_0 and Q_1 states, respectively.
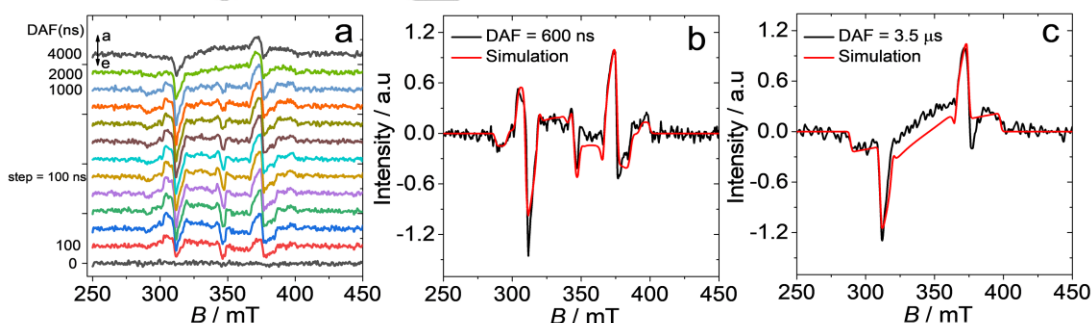
Figure 7. X-band TREPR spectra of **Pery-Ver-1** in frozen toluene at 80 K. (a) Different delay after laser flash from 0 ns to 4000 ns with time window 100 ns (from bottom to top, 9.64 GHz). (b) TREPR spectrum taken at 600 ns along with simulation curve (red line) as the sum of triplet state and quartet state spectra with weights of 0.7 and 0.3, respectively. (c) TREPR spectrum taken at 3.5 µs along with simulation curve (red line) of the triplet state.
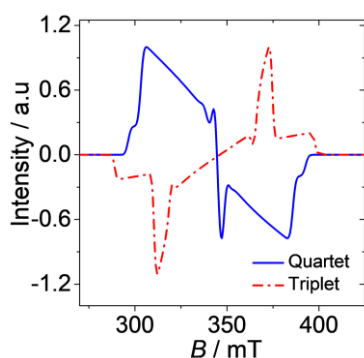
Figure 8. Simulated TREPR spectra of triplet state (red dotted line) and quartet state (blue line) of **Pery-Ver-1**, the sum spectrum of both the states is presented in Figure 8b. Simulation parameters are presented in Table 4.

This difference is reduced in case of **Per-Ver-3**, due to the orientation of the radical unit at 3-C position, the dihedral angle between phenyl ring and verdazyl unit is 5.5° and 7.5° at D_0 and Q_1 sates, respectively. Moreover, the electron density difference maps of D_0 and Q_1 indicate that the electronic coupling between radical and chromophore is not negligible because of π-conjugation between them. The optimized conformation and dihedral angles of the dyads at D_1 state are shown in Figure S38 in the Supporting Information, the dihedral angle values between perylene and phenyl ring attached to verdazyl are 40.8°, 48.2° and 49.7° for **Pery-Ver-1**, **Pery-Ver-2** and **Pery-Ver-3**, respectively. The different geometry of the D_1 and Q_1 states indicates that the electronic coupling between verdazyl and perylene may be different.

Table 3. TREPR simulation parameters of **Pery-Ver-1**

States	$\lvert D\rvert$ (MHz)	$\lvert E\rvert$ (MHz)	Sublevels population ratios [a]	g
Quaret (S = 3/2)	675	160	1: 1: 0: 0	2.002
Triplet (S = 1)	1575	80	0.87: 0.13: 0	2.007

[a] Sublevel population ratios denote $P_{-1/2}$: $P_{+1/2}$: $P_{-3/2}$: $P_{+3/2}$ and P_x: P_y: P_z, for the quartet and triplet states, respectively.

These results indicate that the intervening phenyl ring in **Pery-Ver-2** and **Pery-Ver-3** dyads reduce the geometry distortions between ground and excited state, keeping the relative orientation of the two moieties more planar. The higher planarity facilitates the spin-exchange interactions and increases the electronic delocalization.

To investigate the conformational flexibility of **Pery-Ver-1**, the ground doublet (D_0) and excited quartet (Q_1) state potential energy curves (PEC) were studied (Figure 10). At D_0 state, there are two energy minima, with dihedral angles between verdazyl and perylene moieties at 44° and 134°, respectively (Figure 10a), but there is a large energy barrier for rotation between the two energy minima. This energy barrier is much larger than the thermal energy at room temperature, thus at D_0 state, the molecule prefers to adopt
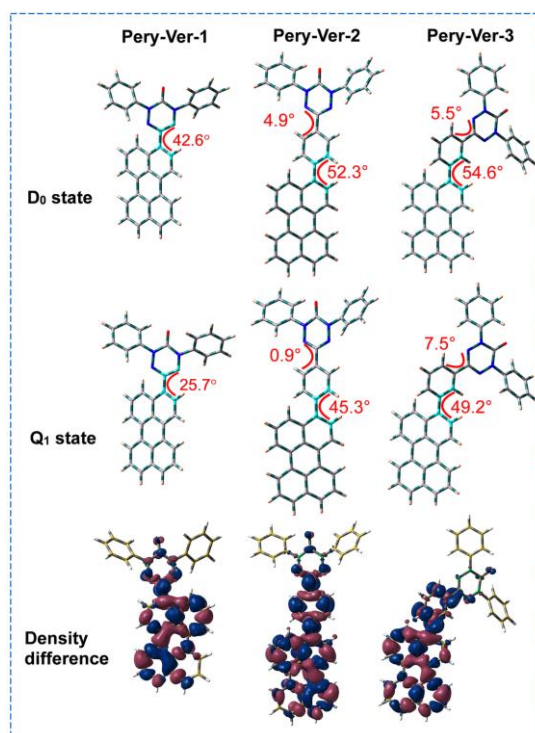
Figure 9. Optimized conformations and the dihedral angles of selected atoms of the radical dyads at doublet (D_0) state and at quartet (Q_1) state. Electronic density difference maps of D_0 and Q_1 states are also presented. Calculated by DFT (UB3LYP/6-31G (d)) using Gaussian 09.

the geometry with a dihedral angle of either 44° or 134°, which is favorable for strong exchange interactions between chromophore and radical. This result is in agreement with the UV/vis absorption and fluorescence emission studies. At Q_1 state (Figure 10b), at room temperature, the PEC also shows two energy minima at 26° and 146°. However, the rotation energy raises sharply when the conformation deviates from the first energy minimum and approaches to the second one at 146°. This result indicates that **Pery-Ver-1** may adopt different geometries also at the excited state, which could be the reason for the observation of triplet and quartet state in TRPER spectroscopy.[60]

We further analyzed the spin density surfaces of the radical compounds in the doublet states (S = 1/2) and the quartet state (S = 3/2).[50,61] For **Pery-Ver-1,** the spin density of the D_0 state (Figure S39 in the Supporting Information) is mostly localized on the radical part but also leaked to the perylene moiety, while for the quartet state the spin density is fully confined on the entire molecule (Figure 11).[61] In the quartet state (Figure 11a), the larger portion of spin density is localized on the perylene moiety, indicating that a larger amount of unpaired spin exists on the perylene chromophore. The excited quartet state is associated to a HOMO-$\alpha \rightarrow$ LUMO-α ($\pi-\pi^*$) transition of the perylene moiety. These results are in accordance with the experimental observations, implying that the $\pi\pi^*$ excited triplet state of perylene is coupled with the doublet spin of
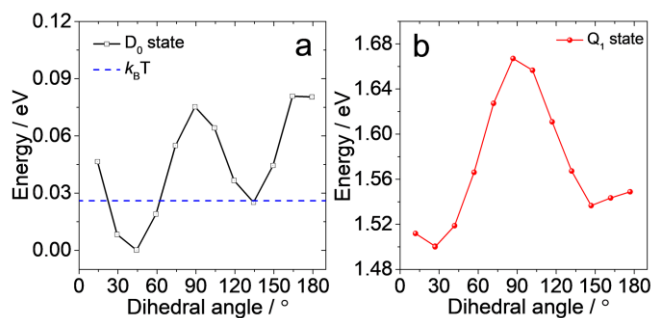
Figure 10. Potential energy curves of **Pery-Ver-1** (a) at doublet (D_0) state and (b) at quartet (Q_1) state as a function of torsion angle between perylene and verdazyl radical. The blue dashed line in (a) represents the thermal energy at room temperature (0.026 eV). Calculated by UB3LYP/6-31G (d) using Gaussian 09.

verdazyl radical. Unequal distribution of positive and negative spin densities over the entire molecule and localization of large positive spin density on the perylene moiety show that the spin delocalization effect vanquishes the spin polarization effect on perylene chromophore. Thus, ferromagnetic exchange interaction between triplet excited state of perylene and the unpair spin of verdazyl radical is realized.
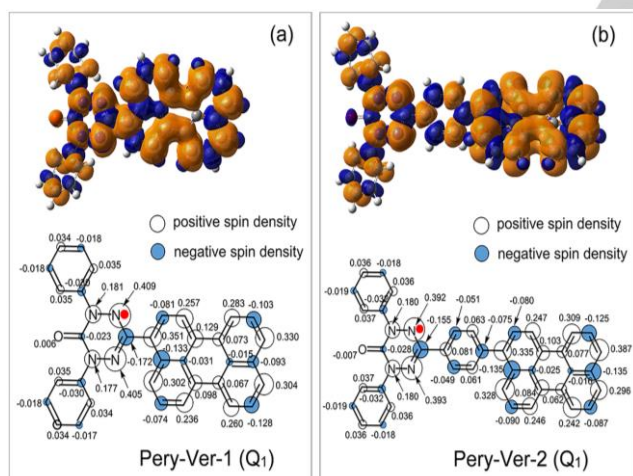
Figure 11. Spin density distribution at lowest optimized quartet excited state (Q1) (a) **Pery-Ver-1** (b) **Pery-Ver-2** obtained by UB3LYP/6-31G (d) level using Gaussian 09.

The Bader Quantum Theory Atoms in Molecules (QTAIM) can provide a good investigation of a π-electron structure in the sense of electron density properties.[62] Concerning the verdazyl moiety, the positive spin density lies largely on the four N atoms and also delocalizes over the π system of the two phenyl rings linked to the N atoms. Due to lone pairs of electrons, the N atoms that are not directly connected to the phenyl rings and have a slightly larger spin density. The negative spin density is indicative of spin polarization, the electron pairs in closer vicinity to the unpaired electron

become more polarized than those further away, added that the two moieties are connected through the spin-polarization mechanism. This large spin polarization effect through π-conjugation leads to a ferromagnetic spin coupling between the excited triplet spins and the verdazyl radical, giving the high-spin states.

For **Pery-Ver-2**, with the phenyl moiety present between the two units, the spin density is localized on radical part in the D_0 state, however, there is a leakage on the phenyl ring (Figure S39, Supporting Information). In the quartet state, the spin density is spread on the whole molecule (Figure 11b). When a phenyl ring is present between perylene and verdazyl the positive and negative density sites become alternatives to each other within the phenyl ring. This spin density distribution suggests that the spin polarization mechanism vanquishes the spin delocalization effect within the phenyl spacer also in the excited state. The verdazyl radical spin couples ferromagnetically through the phenyl spin polarization to the large positive spins of the excited triplet state of perylene, forming the excited quartet state. Similar results were observed for **Pery-Ver-3** (Figure S40 in the Supporting Information). These results are different from what was previously reported in case of the fused perylene-NO• compound, where the excited triplet state decay is fast ($\tau_T = 0.1$ μs).[26]

On the basis of the energy levels of excited doublet and quartet states, we constructed the energy diagram of **Pery-Ver-1** (Figure S41, Supporting Information). We found that the interaction between doublet state of the verdazyl radical and the triplet state of perylene chromophore is ferromagnetic, i.e. $J > 0$. For **Pery-Ver-1**, the D_1 state energy level (1.66 eV) is higher than the Q_1 state (Table S2 and Figure S41, in the Supporting Information), and the calculated J value is 0.05 eV. For **Pery-Ver-2**, the calculated $J = 0.10$ eV is higher than **Pery-Ver-1**. Similar results were observed for **Pery-Ver-3**. The proposed energy diagrams for **Pery-Ver-2** and **Pery-Ver-3** and related parameters are supplied in Figures S42, S43 and Tables S3 and S4 in the Supporting Information. These results are in agreement with previously reported compounds, such as anthracene-oxoverdazyl ($J = 0.015 \sim 0.047$ eV),[37] NDI-verdazyl ($J = 0.07 \sim 0.13$ eV)[41] and pyrene-verdazyl ($J = 0.62$ eV).[50]

The photophysical processes occurring in **Pery-Ver-1** dyad can be understood from Scheme 2. Photoexcitation brings the system to the excited doublet state D_3 instead of D_2 in which the electrons are confined on the perylene unit.[57] From there, either an ultrafast internal conversion towards the lower energy D_2 state (not resolved by transient absorption spectroscopy, but possibly occurring at a time scale faster than the time resolution of the measurement) or direct REISC can occur. REISC is experimentally observed on a sub-picosecond timescale, leading to the formation of a
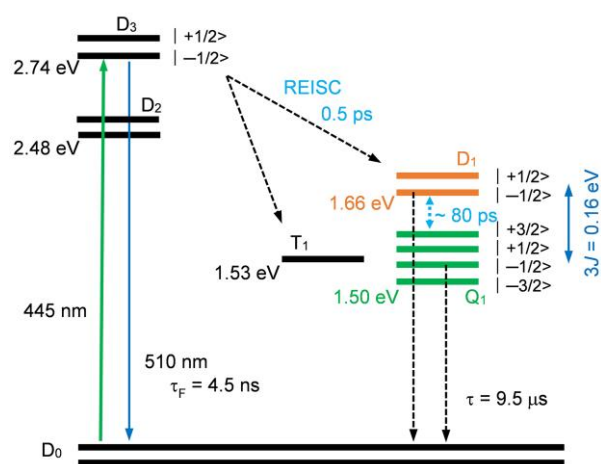
Scheme 2. Energy diagram showing the photophysical process of **Pery-Ver-1.** The energy levels of the excited state are derived from the spectroscopic data and by DFT calculations. The T_1 state energy level is the lowest triplet state of perylene. *D* stands for doublet states and *Q* stands for quartet state. The numbers in subscripts indicate the spin multiplicity of the respective state. For clarity, the excited states are not put in energy scales.

three-spin system in which the perylene is in its triplet state. The interaction between the perylene triplet and the verdazyl radical, which is in a doublet state, results in the formation of an excited doublet (D_1) and quartet (Q_1) states. In this case, we observed both perylene triplet and quartet state in TREPR spectra (the possible path of T_1 state formation is also shown). We did not observe the D_1 state, which lies above the Q_1 state (maybe decays much faster). With nanosecond transient absorption spectroscopy, a long-lived triplet state was observed. By fs-TA the interconversion or equilibrium among the two states ($D_1 \leftrightarrow Q_1$) is observed within ~ 80 ps timescale because D_1 and Q_1 state share almost similar energy. Since the overall spin multiplicity does not change during transitions among doublet states, the perylene ISC process can be ultrafast (< 1.0 ps), although the D_1 state is absent in TREPR.

3. Conclusion

In summary, we prepared perylene-verdazyl radical dyads, in which the verdazyl radical is linked to a perylene chromophore through a single C−C bond or through an intervening phenyl moiety. The photophysical properties of the dyads were studied with steady-state and femtosecond fluorescence up-conversion, nanosecond/femtosecond transient absorption spectroscopic methods, cyclic voltammetry, time-resolved electron paramagnetic resonance (TREPR) spectra as well as DFT computations. We found that the fluorescence quantum yield significantly decreased in the radical compounds (Φ_F = 0.9 ~ 1.5%), as compared to the native perylene (Φ_F = 94%), because of a strong spin-spin interaction between the radical and the

perylene moiety. With femtosecond fluorescence up-conversion and femtosecond transient absorption spectroscopy, we confirmed ultrafast ISC (within 0.5 ps) occurring in these dyads. Interestingly, by fs-TA study, we found the interconversion of the two states (probably doublet and quartet) at 80 ps timescale. Furthermore, cyclic voltammetry studies show that the charge separation is thermodynamically allowed, but the radical enhanced ISC is a faster process, thus no CS state was observed in the fs TA, suggesting that this process is not involved in ISC. Nanosecond transient absorption spectroscopy indicated that the triplet state lifetime of the dyads is much longer (9.5 μs) as compared with that of the previously reported fused perylene-NO• radical system (0.1 μs). The strongly quenched fluorescence and the low triplet state yields (Φ_Δ = 7%) of the dyads indicate that radical-induced internal conversion also plays a significant role in the relaxation of the excited states. Interestingly, with TREPR spectra, we observed mixed triplet and quartet states with a weight factor of 0.7 and 0.3, respectively. The potential energy curve indicates two energy minima, thus the dyad can adopt different geometries upon excitation, which could be the reason for the observation of quartet and triplet states in TREPR spectra. DFT calculations further suggest ferromagnetic interaction between the verdazyl radical and the perylene triplet state (J > 0, 0.05 ~ 0.10 eV). These findings are important for study of the photochemistry of radical labeled chromophore systems, as well as for the design of new heavy atom-free triplet photosensitizers.

Experimental Section

Materials and Methods

All the chemicals used in the synthesis are analytically pure and were used as received. Solvents were dried prior to use. UV/vis absorption spectra were measured on a UV 2550 spectrometer (Shimadzu Ltd, Japan). Fluorescence emission spectra were acquired with an RF-5301PC spectrofluorometer (Shimadzu Ltd, Japan). Fluorescence lifetimes (τ_F) were measured on an OB920 luminescence lifetime spectrometer (with Time-Correlated Single Photon Counting (TCSPC) detection mode. Edinburgh Instruments Ltd., U.K.). For perylene, fluorescence lifetimes were measured with 400 nm EPL picosecond pulsed laser and for radical dyads (**Pery-Ver-1, Pery-Ver-2** and **Pery-Ver-3**) the luminescence lifetimes were measured with 445 nm EPL picosecond pulsed laser excitation.

Synthesis of Compounds

The synthesis and characterization of reference compounds (**Per-Ph**, **Ph-Ver**) and intermediate compounds are provided in Supporting Information.

Synthesis of Pery-Ver-1

Under N_2 atmosphere, compound **2** (112.0 mg, 0.44 mmol) and compound 3 (100.0 mg, 0.44 mmol) were dissolved in dry methanol (12 mL). After complete evacuation of oxygen, pyridium-4-toluene sulfonate (28.0 mg, 0.11 mmol) was added in the reaction mixture and refluxed for 2 h at 70 °C. The reaction was monitored by TLC. After completion of reaction, the solvent was evaporated under reduced pressure and the crude product was used in the next step without purification. In the next step, the crude product was dissolved in dry toluene (7 mL) and *p*-benzoquinone (54.0 mg, 0.5 mmol) was added. Afterward, the reaction mixture was refluxed for 1 h at 80 °C. On completion of reaction, the solvent was dried by evaporation under vacuum and the crude product was purified by column chromatography (silica gel, DCM/*n*-hexane = 1:2, v/v) to obtain a reddish-brown solid (60.0 mg, yield: 27%). mp > 250 °C. TOF-MALDI-HRMS: Calcd ([$C_{34}H_{21}N_4O^\bullet$]$^-$), *m/z* = 501.1715; found, *m/z* = 501.1720. FTIR (KBr): $\tilde{v}$ = 3433.02, 2959.37, 2924.68, 2854.49, 1730.26, 1704.56, 1460.21, 1381.11, 1122.22, 807.88, 754.07, 688.65, 470.21 cm^{-1}. Elemental analysis calcd for [$C_{34}H_{21}N_4O^\bullet$ + 0.99 C_7H_8 + 0.14 CH_2Cl_2]: C, 81.58; H, 4.87; N, 9.27. Found: C, 81.93; H, 4.25; N, 8.80.

Synthesis of Pery-Ver-2

Under N_2 atmosphere, compound **6** (115.4 mg, 0.2 mmol) was dissolved in dry toluene (10 mL) after evacuation of oxygen, followed by the addition of 1, 4-benzoquinone (64.8 mg, 0.6 mmol). Then the reaction mixture was refluxed for 1.5 h at 80 °C, and color changed from yellowish orange to dark reddish brown. On completion of the reaction, solvent was dried by evaporation under vacuum and the crude product was purified by column chromatography (silica gel, DCM/*n*-hexane = 1:3, v/v) to obtain a dark red solid (40.0 mg, yield: 31.4%). mp > 250 °C. TOF-ESI-HRMS: Calcd ([$C_{40}H_{25}N_4O^\bullet$]$^+$) *m/z* = 577.2028; found, *m/z* = 577.2041. FTIR (KBr): $\tilde{v}$ = 3434.01, 3044.11, 2921.13, 2850.53, 1697.33, 1489.99, 1386.29, 1243.80, 1123.50, 808.49, 749.16, 684.06, 601.40, 505.36 cm^{-1}. Elemental analysis calcd for [$C_{40}H_{25}N_4O^\bullet$ + 0.10 CH_2Cl_2]: C, 82.17; H, 4.33; N, 9.56. Found: C, 82.47; H, 4.58; N, 9.16.

Synthesis of Pery-Ver-3

Pery-Ver-3 was synthesized by following the same method as for **Pery-Ver-2**. The product was obtained as red solid (44.0 mg, yield: 34.6%). mp > 250 °C. TOF-ESI-HRMS: Calcd ([$C_{40}H_{25}N_4O^\bullet$]$^+$), *m/z* = 577.2028; found, *m/z* = 577.2031. IR (KBr): $\tilde{v}$ = 3432.18, 3044.70, 2920.95, 2851.38, 1695.85, 1491.39, 1387.19, 1232.79, 1123.98, 807.16, 748.85, 681.83, 606.80, 505.68 cm^{-1}. Elemental analysis calcd for [$C_{40}H_{25}N_4O^\bullet$ + 0.14 CH_2Cl_2]: C, 81.78; H, 4.32; N, 9.50. Found: C, 82.10; H, 4.55; N, 9.09.

Time-Resolved Fluorescence Up-Conversion Spectroscopy

The short-living fluorescence lifetimes components were recorded with a time-resolved fluorescence spectrometer (Newport) in combination with a mode-locked Ti-sapphire laser (Mai Tai DeepSee, Spectra-Physics). The femtosecond laser system generated light pulses at 800 nm of duration 150 fs at a repetition rate of 80 MHz and average power 2.9 W. The frequency of the laser pulse was doubled with a BBO crystal and served for excitation. The residual fundamental pulse, used as a gate pulse, was split from the pump beam with a beam splitter. The intensity of the excitation beam at 400 nm excitation wavelength was kept below 20 mW in order to avoid photochemical degradation of the sample. The measurements were carried out in a 1 mm cuvette. The polarization of the excitation and gate beams were set at a magic angle (55°) in order to eliminate the contributions of the rotational diffusion. The emitted fluorescence was collected by a lens and focused on a BBO crystal together with the 800 nm gate beam to create the up-converted signal via sum-frequency generation (SGF). The resulting sum-frequency radiation was focused onto the entrance slit of a monochromator. The overall time resolution of the setup was 100 fs.

Nanosecond Transient Absorption Spectroscopy

LP980 laser flash-photolysis spectrometer (Edinburgh Instruments, Ltd., UK) equipped with Tektronix TDS 3012B oscilloscope was used to study the nano- and microsecond dynamics. The samples were purged with N_2 for 15-20 minutes before measurement, and excited with a nanosecond pulsed laser (Opolette^{TM} 355II+UV nanosecond pulsed laser, the wavelength is tunable in the range of 200−2200 nm. OPOTEK, USA). In order to enhance the signal-to-noise ratio, the collinear setup of the pump/probe beams was used for measurements. The nanosecond transient absorption of the reference compounds (perylene, compound **6** and compound **8**) was measured by intermolecular triplet photosensitizing method (TTET), and the triplet spectra were analyzed with the global fitting method.

Femtosecond Transient Absorption Spectroscopy

A system based on Ti:sapphire regenerative amplifier (BMI Alpha 1000) pumped by a Ti:sapphire oscillator (Spectra Physics Tsunami) was used for fs-TA study, with 150 fs time resolution. The system produces 100-fs pulses at 785 nm, with a repetition rate of 1 kHz and average power of 450-500 mW. Excitation pulses at 400 nm were obtained by second-harmonic generation of the fundamental laser output through a BBO crystal. The probe pulses were generated by focusing a small portion of the fundamental laser output radiation on a 3 mm thick calcium fluoride

window. The pump beam polarization has been set to the magic angle with respect to the probe beam by rotating a λ/2 plate. Pump-probe delays were introduced by using a motorized stage, which allowed to record pump-probe spectra up to 1.5 ns time delay. The transient signal was revealed by sending the probe beam to a flat field monochromator coupled to a CCD detector. The measurements were carried out in a quartz cell (2 mm thick) mounted on a movable stage to avoid sample photo-degradation and multiple-photo excitation of the solution. The recorded transient absorption spectra have been analyzed by using a global-fitting and target analysis procedure using the GLOTARAN software.[63]

Continuous-Wave Electron Paramagnetic Resonance and Time-Resolved Electron Paramagnetic Resonance Spectroscopy

CW-EPR spectra were recorded at room temperature using an Elexsys E-580 spectrometer (Bruker) at the X-band, with a 100 kHz field modulation.

TREPR spectral measurements were carried out at 80 K. The samples were excited at 450 nm (1 mJ pulse,10 ns, 100 Hz) using the output of an optical parametric oscillator (LP603 SOLAR Laser Systems), pumped with the output of a Nd:YAG laser (LQ629 SOLAR Laser Systems). The measurements were done in frozen solution (ca. 10^{-4} M) and loaded in quartz tube (4.8 mm o.d × 2.8 mm i.d). Bruker Elexsys E580 EPR spectrometer with a flexlinel resonator (ER 4118X-MD5-W1) at X-band (9.67 GHz) frequencies was used. The TR CW EPR spectra were obtained by the summation of the data in different time windows after the laser pulse. The EPR spectra were simulated using the Easy Spin package implemented in the MATLAB programming language.[64]

Echo-detected transient nutation was performed by echo detection of longitudinal magnetization after a nutation pulse. Length of $\pi/2$ pulse is 16 ns, delay between $\pi/2$ and π pulses (τ) is 140 ns.

Keywords: electron spin polarization • perylene • radical-enhanced intersystem crossing • spin-spin exchange • triplet state

[1] S. K. Chattopadhyay, P. K. Das, G. L. Hug, *J. Am. Chem. Soc.* **1983**, *105*, 6205–6210.
[2] A. Kawai, K. Obi, *J. Phys. Chem.* **1992**, *96*, 52–56.
[3] C. K. Prier, D. A. Rankic, D. W. C. MacMillan, *Chem. Rev.* **2013**, *113*, 5322–5363.
[4] J. Xuan, W.-J. Xiao, *Angew. Chem. Int. Ed.* **2012**, *51*, 6828–6838.
[5] J. Zhao, S. Ji, W. Wu, W. Wu, H. Guo, J. Sun, H. Sun, Y. Liu, Q. Li, L. Huang, *RSC Adv.* **2012**, *2*, 1712–1728.
[6] E. Cló, J. W. Snyder, P. R. Ogilby, K. V. Gothelf, *ChemBioChem.* **2007**, *8*, 475–481.
[7] Z. Wang, Y. Gao, M. Hussain, S. Kundu, V. Rane, M. Hayvali, E. A. Yildiz, J. Zhao, H. G. Yaglioglu, R. Das, L. Luo, J. Li, *Chem. – Eur. J.* **2018**, *24*, 18663–18675.
[8] X. Li, S. Kolemen, J. Yoon, E. U. Akkaya, *Adv. Funct. Mater.* **2017**, *27*, 1604053.
[9] P. Majumdar, R. Nomula, J. Zhao, *J. Mater. Chem. C.* **2014**, *2*, 5982–5997.
[10] A. Kamkaew, S. H. Lim, H. B. Lee, L. V. Kiew, L. Y. Chung, K. Burgess, *Chem. Soc. Rev.* **2013**, *42*, 77–88.
[11] T. N. Singh-Rachford, F. N. Castellano, *Coord. Chem. Rev.* **2010**, *254*, 2560–2573.
[12] P. Ceroni, *Chem. – Eur. J.* **2011**, *17*, 9560–9564.
[13] Z. Wang, J. Zhao, A. Barbon, A. Toffoletti, Y. Liu, Y. An, L. Xu, A. Karatay, H. G. Yaglioglu, E. A. Yildiz, M. Hayvali, *J. Am. Chem. Soc.* **2017**, *139*, 7831–7842.
[14] A. Monguzzi, R. Tubino, S. Hoseinkhani, M. Campione, F. Meinardi, *Phys. Chem. Chem. Phys.* **2012**, *14*, 4322–4332.
[15] J. Zhao, S. Ji, H. Guo, *RSC Adv.* **2011**, *1*, 937–950.
[16] R. P. Sabatini, T. M. McCormick, T. Lazarides, K. C. Wilson, R. Eisenberg, D. W. McCamant, *J. Phys. Chem. Lett.* **2011**, *2*, 223–227.
[17] J. Zhao, K. Xu, W. Yang, Z. Wang, F. Zhong, *Chem. Soc. Rev.* **2015**, *44*, 8904–8939.
[18] W. Pang, X.-F. Zhang, J. Zhou, C. Yu, E. Hao, L. Jiao, *Chem. Commun.* **2012**, *48*, 5437–5439.
[19] V. Bandi, H. B. Gobeze, V. Lakshmi, M. Ravikanth, F. D'Souza, *J. Phys. Chem. C.* **2015**, *119*, 8095–8102.
[20] M. A. Filatov, S. Karuthedath, P. M. Polestshuk, H. Savoie, K. J. Flanagan, C. Sy, E. Sitte, M. Telitchko, F. Laquai, R. W. Boyle, M. O. Senge, *J. Am. Chem. Soc.* **2017**, *139*, 6282–6285.
[21] L. Huang, X. Cui, B. Therrien, J. Zhao, *Chem. – Eur. J.* **2013**, *19*, 17472–17482.
[22] K. Feng, M.-L. Yu, S.-M. Wang, G.-X. Wang, C.-H. Tung, L.-Z. Wu, *ChemPhysChem.* **2013**, *14*, 198–203.
[23] J. Zhao, W. Wu, J. Sun, S. Guo, *Chem. Soc. Rev*, **2013**, *42*, 5323–5351.
[24] N. J. Turro, V. Ramamurthy, J. C. Scaiano, *Principles of Molecular Photochemistry: An Introduction*, University Science Books, Sausalito, CA, **2009**.
[25] E. M. Giacobbe, Q. Mi, M. T. Colvin, B. Cohen, C. Ramanan, A. M. Scott, S. Yeganeh, T. J. Marks, M. A. Ratner, M. R. Wasielewski, *J. Am. Chem. Soc.* **2009**, *131*, 3700–3712.
[26] S. M. Dyar, E. A. Margulies, N. E. Horwitz, K. E. Brown, M. D. Krzyaniak, M. R. Wasielewski, *J. Phys. Chem. B.* **2015**, *119*, 13560–13569.
[27] K. Kanemoto, A. Fukunaga, M. Yasui, D. Kosumi, H. Hashimoto, H. Tamekuni, Y. Kawahara, Y. Takemoto, J. Takeuchi, Y. Miura, Y. Teki, *RSC Adv.* **2012**, *2*, 5150–5153.
[28] A. Ito, N. Kobayashi, Y. Teki, *Inorg. Chem.* **2017**, *56*, 3794–3808.
[29] B. K. Hughes, W. A. Braunecker, A. J. Ferguson, T. W. Kemper, R. E. Larsen, T. Gennett, *J. Phys. Chem. B.* **2014**, *118*, 12541–12548.

[30] D. Matuschek, S. Eusterwiemann, L. Stegemann, C. Doerenkamp, B. Wibbeling, C. G. Daniliuc, N. L. Doltsinis, C. A. Strasser, H. Eckert, A. Studer, *Chem. Sci.* **2015**, *6*, 4712–4716.

[31] Y. Teki, S. Miyamoto, M. Nakatsuji, Y. Miura, *J. Am. Chem. Soc.* **2001**, *123*, 294–305.

[32] K. Ishii, Y. Hirose, N. Kobayashi, *J. Phys. Chem. A.* **1999**, *103*, 1986–1990.

[33] Y. Teki, H. Tamekuni, K. Haruta, J. Takeuchi, Y. Miura, *J. Mater. Chem.* **2008**, *18*, 381–391.

[34] S. E. Herbelin, N. V. Blough, *J. Phys. Chem. B.* **1998**, *102*, 8170–8176.

[35] N. Medvedeva, V. V. Martin, A. L. Weis, G. I. Likhtenshten, *J. Photochem. Photobio. Chem.* **2004**, *163*, 45–51.

[36] E. Sartori, A. Toffoletti, C. Corvaja, L. Moroder, F. Formaggio, C. Toniolo, *Chem. Phys. Lett.* **2004**, *385*, 362–367.

[37] I. Matsumoto, I. Ciofini, P. P. Lainé, Y. Teki, *Chem. – Eur. J.* **2009**, *15*, 11210–11220.

[38] T. Yoshio, K. Mituhiro, N. Shinsuke, O. Keishi, M. Kazuo, *Bull. Chem. Soc. Jpn.* **2004**, *77*, 95–99.

[39] D. Schmidt, M. Son, J. M. Lim, M.-J. Lin, I. Krummenacher, H. Braunschweig, D. Kim, F. Würthner, *Angew. Chem. Int. Ed.* **2015**, *54*, 13980–13984.

[40] K. Xu, A. A. Sukhanov, Y. Zhao, J. Zhao, W. Ji, X. Peng, D. Escudero, D. Jacquemin, V. K. Voronkova, *Eur. J. Org. Chem.* **2018**, *2018*, 885–895.

[41] M. Hussain, M. Taddei, L. Bussotti, P. Foggi, J. Zhao, Q. Liu, M. Di Donato, *Chem. – Eur. J.* **2019**, *25*, 15615–15627.

[42] J. M. Giaimo, J. V. Lockard, L. E. Sinks, A. M. Scott, T. M. Wilson, M. R. Wasielewski, *J. Phys. Chem. A.* **2008**, *112*, 2322–2330.

[43] R. E. Cook, B. T. Phelan, R. J. Kamire, M. B. Majewski, R. M. Young, M. R. Wasielewski, *J. Phys. Chem. A.* **2017**, *121*, 1607–1615.

[44] V. Maurel, M. Laferrière, P. Billone, R. Godin, J. C. Scaiano, *J. Phys. Chem. B.* **2006**, *110*, 16353–16358.

[45] Y. Kandrashkin, A. van der Est, *Chem. Phys. Lett.* **2003**, *379*, 574–580.

[46] A. Kawai, K. Shibuya, *J. Photochem. Photobio C: Photochem. Rev.* **2006**, *7*, 89–103.

[47] K. Chen, J. Zhao, X. Li and G. G. Gurzadyan, *J. Phys. Chem. A.* **2019**, *123*, 2503–2516.

[48] B. Carlotti, M. Poddar, F. Elisei, A. Spalletti, R. Misra, *J. Phys. Chem. C.* **2019**, *123*, 24362–24374.

[49] Y. Zhao, A. A. Sukhanov, R. Duan, A. Elmali, Y. Hou, J. Zhao, G. G. Gurzadyan, A. Karatay, V. K. Voronkova, C. Li, *J. Phys. Chem. C.* **2019**, *123*, 18270–18282.

[50] T. Sadhukhan, A. Datta, S. N. Datta, *J. Phys. Chem. A.* **2015**, *119*, 9414–9424.

[51] Z. Wang, M. Ivanov, Y. Gao, L. Bussotti, P. Foggi, H. Zhang, N. Russo, B. Dick, J. Zhao, M. Di Donato, G. Mazzone, L. Luo, M. Fedin, *Chem. – Eur. J,* **2020**, *26*, 1091–1102.

[52] M. T. Colvin, E. M. Giacobbe, B. Cohen, T. Miura, A. M. Scott, M. R. Wasielewski, *J. Phys. Chem. A.* **2010**, *114*, 1741–1748.

[53] K. Ishii, Y. Hirose, H. Fujitsuka, O. Ito, N. Kobayashi, *J. Am. Chem. Soc.* **2001**, *123*, 702–708.

[54] M. Imran, A. A. Sukhanov, Z. Wang, A. Karatay, J. Zhao, Z. Mahmood, A. Elmali, V. K. Voronkova, M. Hayvali, Y. H. Xing, S. Weber, *J. Phys. Chem. C.* **2019**, *123*, 7010–7024.

[55] J.-i. Fujisawa, Y. Ohba, S. Yamauchi, *J. Phys. Chem. A.* **1997**, *101*, 434–439.

[56] S. Jockusch, O. Zeika, N. Jayaraj, V. Ramamurthy, N. J. Turro, *J. Phys. Chem. Lett.* **2010**, *1*, 2628–2632.

[57] Y. Huang, Z. Xu, S. Jin, C. Li, K. Warncke, F. A. Evangelista, T. Lian, E. Egap, *Chem. Mater.* **2018**, *30*, 7840–7851.

[58] Y. H. Meyer, P. Plaza, *Chem. Phys.* **1995**, *200*, 235–243.

[59] C. R. Goldschmidt and M. Ottolenghi, *J. Phys. Chem.* **1971**, *75*, 3894–3897.

[60] K. Ishii, T. Ishizaki, N. Kobayashi, Appl. Magn. Reson. **2003**, 23, 369.

[61] Y. Teki, M. Nakatsuji and Y. Miura, *Molecul Phys.* **2002**, *100*, 1385–1394.

[62] R. F. W. Bader, *Atoms in Molecules: A Quantum Theory*, Oxford University Press, New York, **1990**.

[63] I. H. M. van Stokkum, D. S. Larsen and R. van Grondelle, *Biochim. Biophys. Bioenerge.* **2004**, *1657*, 82–104.

[64] S. Stoll, A. Schweiger, *J. Magn. Reson.* **2006**, 178, 42-55.

WILEY-VCH

Entry for the Table of Contents

RESEARCH ARTICLE

Long-lived triplet excited state (τ_T = 9.5 μs) was observed for verdazyl radical-perylene dyads. Spin-spin exchange interaction between perylene chromophore and verdazyl moiety is responsible for the triplet population. The interconversion among the two states (doublet and quartet) in 80 ps was observed with femtosecond transient absorption. By TREPR spectra, quartet and triplet states were observed simultaneously.

Radical-Enhanced ISC in Perylene-Verdazyl Dyads

Muhammad Imran, Maria Taddei, Andrey A. Sukhnov, Laura Bussotti, Wenjun Ni, Paolo Foggi, Gagik G. Gurzadyan, Jianzhang Zhao*, Mariangela Di Donato*, Violeta K. Voronkova*

1 – 14

Radical-Enhanced Intersystem Crossing in Perylene-Oxoverdazyl Radical Dyads

Institute and/or researcher Twitter usernames: @imraan756